Contents

List of Figures

List of Tables

1 Objectives

1. **Determination of Buckling Loads:**
    - Investigate and quantify the buckling loads of slender pin-ended bars through experimental procedures.
    - Analyze the relationship between applied loads and the resulting center deflections for each tested bar.
2. **Comparison of Theoretical and Experimental Critical Loads:**
    - Assess and calculate the theoretical critical loads for the pin-ended bars using relevant analytical models.
    - Perform experimental tests to determine the critical loads for each bar.
    - Conduct a comprehensive comparison between the theoretical predictions and the experimentally obtained critical loads for all tested bars.

Through these objectives, the aim is to enhance our understanding of the buckling behavior of slender pin-ended bars and to evaluate the accuracy of theoretical predictions in relation to practical experimental outcomes.

2 Procedure

1. **Bar Insertion and Setup:**
    - Insert one of the bars between the supports, ensuring that the ball bearing at the ends seats firmly.
    - Orient the larger dimension of the cross-section parallel to the floor.
    - Position the displacement transducer to measure the vertical deflection of the bar.
2. **Moment of Inertia Calculation and Critical Load Prediction:**
    - Calculate the minimum moment of inertia for the inserted bar.
    - Predict the critical load for the bar based on the calculated moment of inertia.
3. **Data Collection Using Dalite Datascan Configurator:**
    - Open the Dalite Datascan Configurator at the DB2Bc.OVL file.
    - Click on the "monitor every second" window.
    - Verify that the initial reading for the electrical potentiometer is zero.
    - Apply the load increments slowly.
    - At each increment, record the central deflection.
    - Continue to increase the load until the column buckles or the central deflection becomes large.
4. **Repeat for All Bars:**
    - Repeat steps 2 to 4 for all four bars in the experimental setup.

This procedure outlines the steps to insert the bars, calculate relevant parameters, and conduct the experimental testing using the Dalite Datascan Configurator. It ensures systematic data collection for each bar in the study.

3 Results

3.1 Plot Calibration Charts

The calibration charts for the load cell and the displacement transducer are shown in the subsequent figures. The calibration charts are used to determine the equation of the line of best fit for the data points. The equation is then used to calculate the load for any pressure values that exceeded those for which the corresponding load is provided.

3.1.1 Bar 1: 508 mm

The calibration chart for the load cell of Bar 1 with 508 mm length is shown in figure 1 along with the equation of the line of best fit.

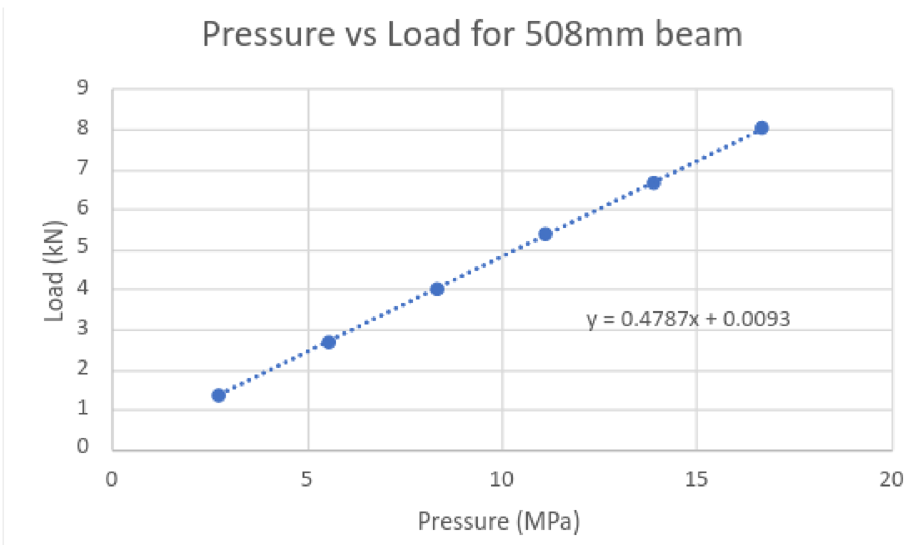

Figure 1: Bar 1 Calibration Chart

3.1.2 Bar 2: 737 mm

The calibration chart for the load cell of Bar 2 with 737 mm length is shown in figure 2 along with the equation of the line of best fit.

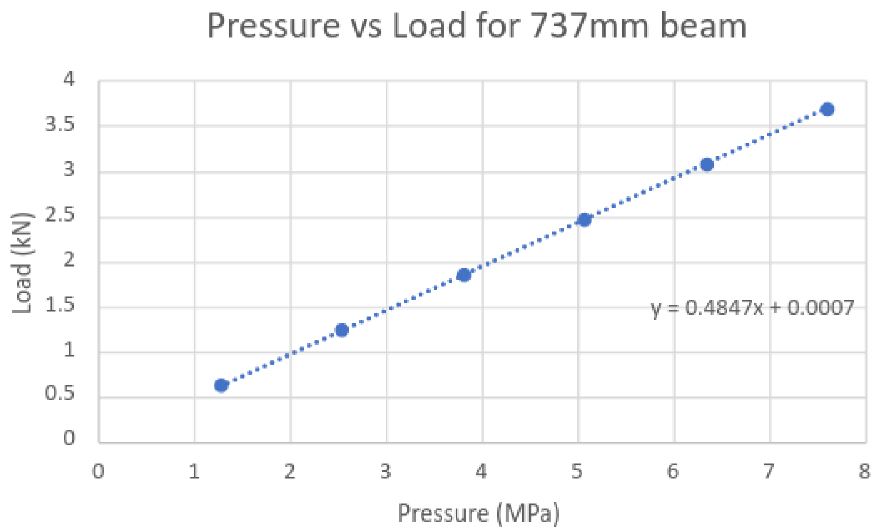

Figure 2: Bar 2 Calibration Chart

3.1.3 Bar 3: 902 mm

The calibration chart for the load cell of Bar 3 with 902 mm length is shown in figure 3 along with the equation of the line of best fit.

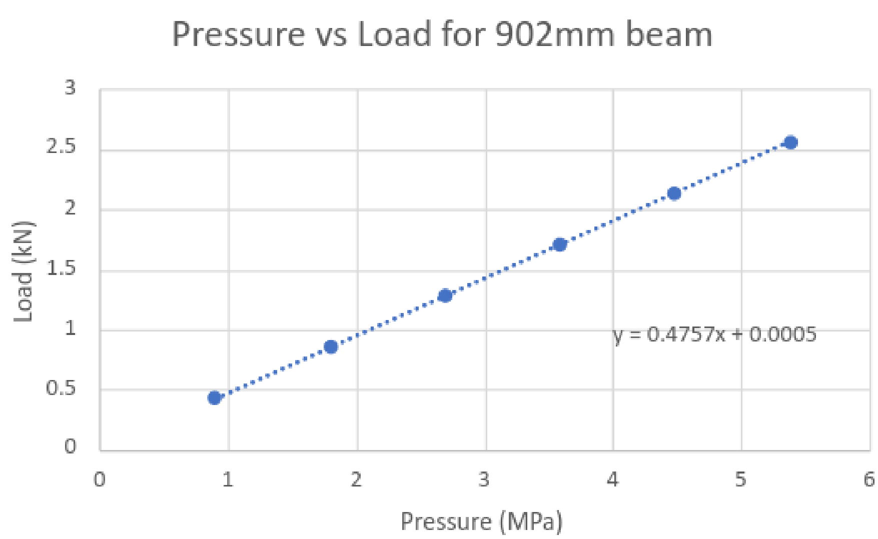

Figure 3: Bar 3 Calibration Chart

3.1.4 Bar 4: 997 mm

The calibration chart for the load cell of Bar 4 with 997 mm length is shown in figure 4 along with the equation of the line of best fit.

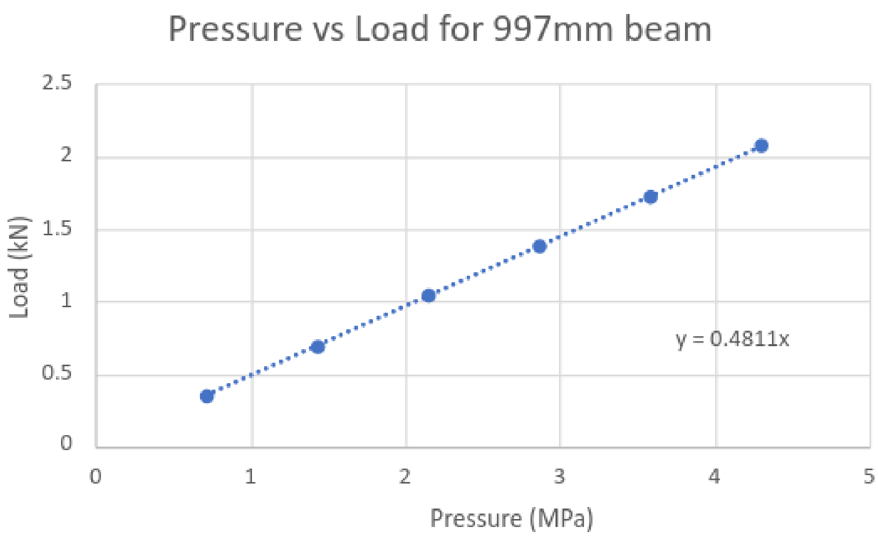

Figure 4: Bar 4 Calibration Chart

3.2 Calculated Pressure for Exceeding Loads

The pressure is calculated using the equation of the line of best fit for the calibration charts. The calculated pressure is shown along with the load and the deflection for each exceeding load in the subsequent tables.

3.2.1 Bar 1: 508 mm

The calculated pressure for the exceeding loads of Bar 1 with 508 mm length is shown in table 1.

Table 1: Bar 1: 508 mm Exceeding Loads

Pressure (MPa)	Load (kN)	Deflection (mm)
2.785481949	1.34	0.3277
5.570963899	2.68	0.7734
8.356445848	4.015	1.271
11.1419278	5.35	1.9436
13.92740975	6.64	2.7734
16.7128917	8.03	4.7394
17.71952626	8.491637222	12.083

3.2.2 Bar 2: 737 mm

The calculated pressure for the exceeding loads of Bar 2 with 737 mm length is shown in table 2.

Table 2: Bar 2: 737 mm Exceeding Loads

Pressure (MPa)	Load (kN)	Deflection (mm)
1.268635343	0.616	0.2422
2.537270687	1.23	0.6727
3.80590603	1.845	1.2167
5.074541373	2.46	1.6104
6.343176716	3.075	2.1479
7.61181206	3.69	2.7867
10.06634566	4.879857741	23.3818

3.2.3 Bar 3: 902 mm

The calculated pressure for the exceeding loads of Bar 3 with 902 mm length is shown in table 3.

Table 3: Bar 3: 737 mm Exceeding Loads

Pressure (MPa)	**Load (kN)**	**Deflection (mm)**
0.896318449	0.427	0.1628
1.792636898	0.853	0.2696
2.688955347	1.28	0.4546
3.585273796	1.707	0.6953
4.481592245	2.13	1.2315
5.377910694	2.56	5.1589
7.322232253	3.483685883	18.8641

3.2.4 Bar 4: 997 mm

The calculated pressure for the exceeding loads of Bar 4 with 997 mm length is shown in table 4.

Table 4: Bar 4: 997 mm Exceeding Loads

Pressure (MPa)	**Load (kN)**	**Deflection (mm)**
0.717054759	0.345	0.1956
1.434109519	0.69	0.6738
2.151164278	1.035	1.0114
2.868219037	1.38	1.3878
3.585273796	1.725	1.9515
4.302328556	2.07	2.4975
6.343176716	3.051702318	20.7397

3.3 Analytical Calculations for Bar 1: 508 mm

The following information is given:

- $A = 12.7\text{mm} \times 19.07 \text{ mm} = 242.489 \text{ mm}^2$
- $E = 70$ GPa
- $L = 508$ mm

3.3.1 Minimum Moment of Inertia

The minimum moment of inertia is calculated using equation 1.

$$I_{min} = \frac{bh^3}{12} \tag{1}$$

Substituting the values in equation 1 yields equation 2.

$$I_{min} = \frac{19.07 \times 12.7^3}{12} = 3255.2219\text{mm}^4 \tag{2}$$

3.3.2 Critical Load

The critical load is calculated using equation 3.

$$P_{cr} = \frac{\pi^2 E I_{min}}{L^2} \tag{3}$$

Substituting the values in equation 3 yields equation 4.

$$P_{cr} = \frac{\pi^2 \times 70 \times 10^9 \times 3255.2219 \times 10^{-12}}{(508 \times 10^{-3})^2} = 8.7146\text{kN} \tag{4}$$

3.3.3 Critical Stress

The critical stress is calculated using equation 5.

$$\sigma_{cr} = \frac{P_{cr}}{A} \tag{5}$$

Substituting the values in equation 5 yields equation 6.

$$\sigma_{cr} = \frac{8.71467 \times 10^3}{242.489} = 35.9829\text{MPa} \tag{6}$$

3.3.4 Radius of Gyration

The radius of gyration is calculated using equation 7.

$$r = \sqrt{\frac{I}{A}} \tag{7}$$

Substituting the values in equation 7 yields equation 8.

$$r = \sqrt{\frac{3255.2219}{242.489}} = 3.66617\text{mm} \tag{8}$$

3.3.5 Slenderness Ratio

The slenderness ratio is calculated using equation 9.

$$\frac{L}{r} = \frac{508}{3.66617} = 138.564 \tag{9}$$

3.4 Plot Load-Deflection Curves

This section shows the load-deflection curves for each bar with an indication of the critical load. Then, the percentage error between the theoretical and experimental critical loads is calculated.

3.4.1 Bar 1: 508 mm

The load-deflection curve for Bar 1 with 508 mm length is shown in figure 5. The theoretical critical load is 8.4916 kN and the experimental critical load is 8.03 kN.

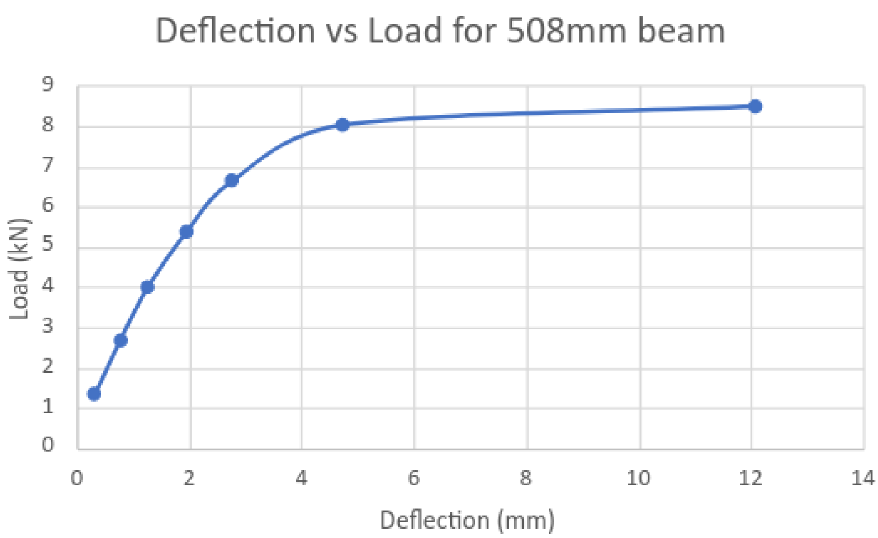

Figure 5: Bar 1: 508 mm Load-Deflection Curve

The percentage error between the theoretical and experimental critical loads is calculated using equation 10 and is shown in equation 11.

$$\text{Percentage Error} = \frac{\text{Experimental} - \text{Theoretical}}{\text{Theoretical}} \times 100 \tag{10}$$

Substituting the values in equation 10 yields equation 11.

$$\text{Percentage Error} = \frac{|8.03 - 8.4916|}{|8.4916|} \times 100 = 5.43\% \tag{11}$$

3.4.2 Bar 2: 737 mm

The load-deflection curve for Bar 2 with 737 mm length is shown in figure 6. The theoretical critical load is 4.8799 kN and the experimental critical load is 3.69 kN.

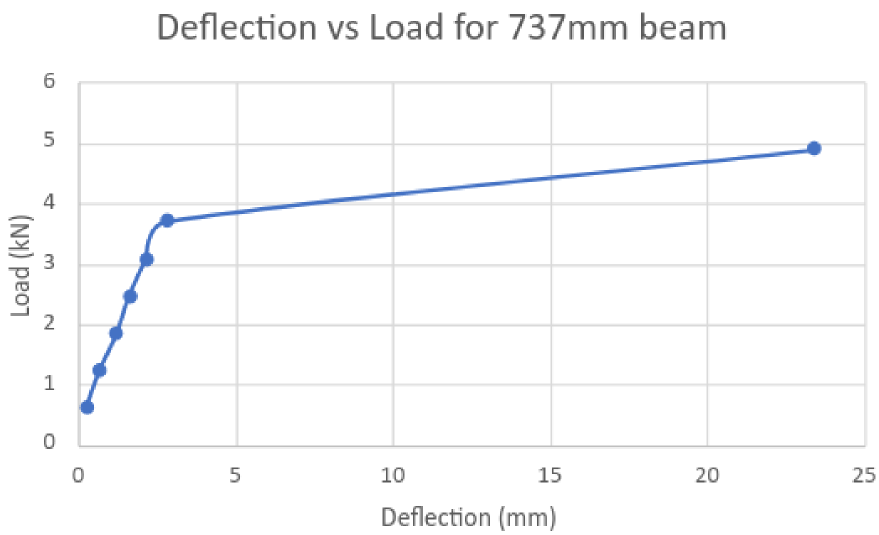

Figure 6: Bar 2: 737 mm Load-Deflection Curve

The percentage error between the theoretical and experimental critical loads is calculated using equation 10 and is shown in equation 12.

$$\text{Percentage Error} = \frac{|3.69 - 4.8799|}{|4.8799|} \times 100 = 24.38\% \tag{12}$$

3.4.3 Bar 3: 902 mm

The load-deflection curve for Bar 3 with 902 mm length is shown in figure 7. The theoretical critical load is 3.4837 kN and the experimental critical load is 2.56 kN.

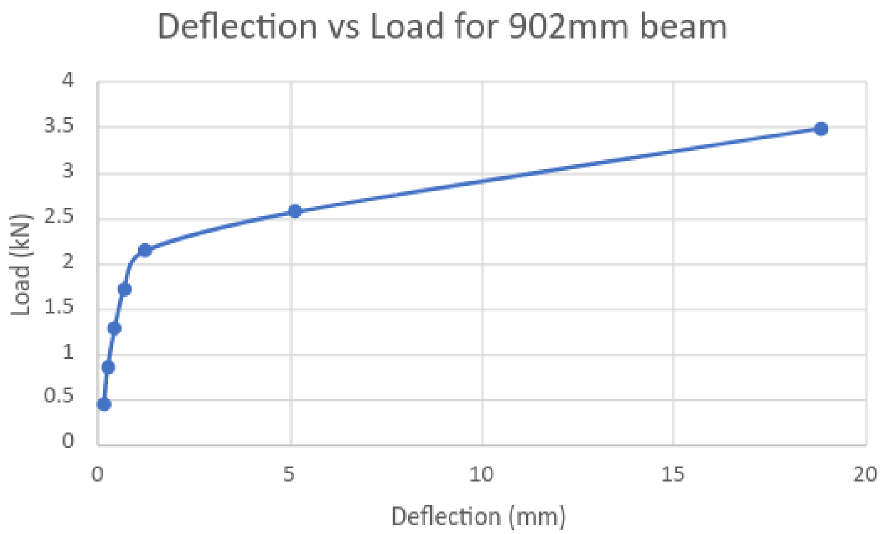

Figure 7: Bar 3: 902 mm Load-Deflection Curve

The percentage error between the theoretical and experimental critical loads is calculated using equation 10 and is shown in equation 13.

$$\text{Percentage Error} = \frac{|2.56 - 3.4837|}{|3.4837|} \times 100 = 26.51\% \tag{13}$$

3.4.4 Bar 4: 997 mm

The load-deflection curve for Bar 4 with 997 mm length is shown in figure 8. The theoretical critical load is 3.0517 kN and the experimental critical load is 2.07 kN.

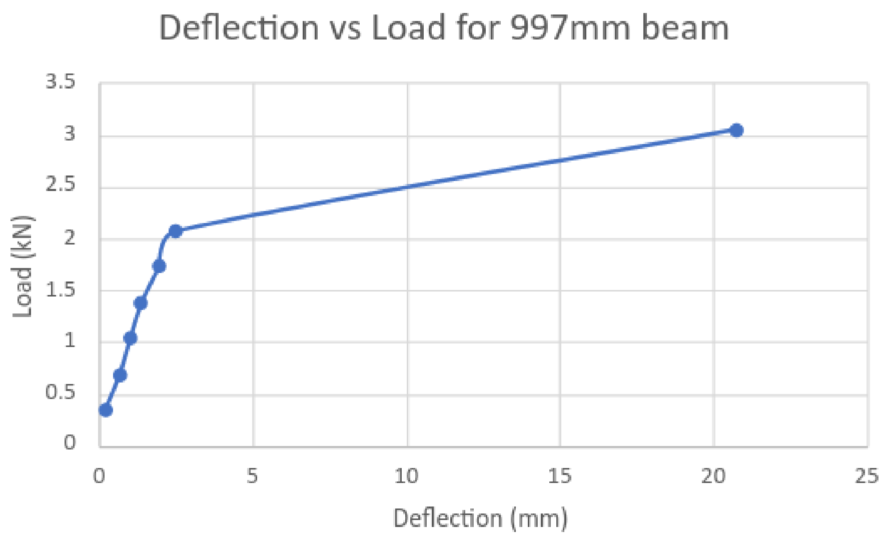

Figure 8: Bar 4: 997 mm Load-Deflection Curve

The percentage error between the theoretical and experimental critical loads is calculated using equation 10 and is shown in equation 14.

$$\text{Percentage Error} = \frac{|2.07 - 3.0517|}{|3.0517|} \times 100 = 32.13\% \tag{14}$$

3.5 Plot Critical Stress-Slenderness Ratio Curves

This section shows the critical stress-slenderness ratio curves for each bar for both the theoretical and experimental values in a single plot. The plot is shown in figure 9.

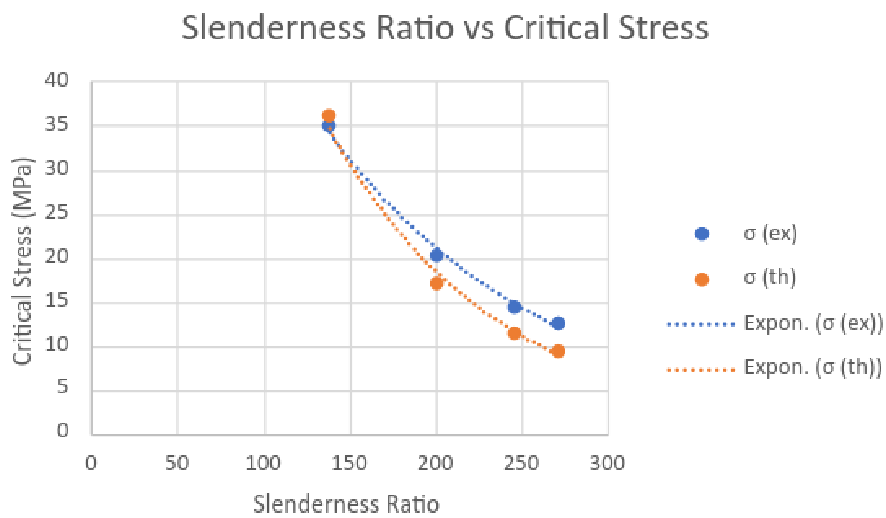

Figure 9: Critical Stress-Slenderness Ratio Curves

3.6 Summary of Results

In this section, the pertinent results of the experiment are summarized in a table. The table includes (L, $\frac{L}{r}$, $P_{cr,theo}$, $P_{cr,exp}$, $\sigma_{cr,theo}$, $\sigma_{cr,exp}$, and % Error). The summary table is shown in table 5.

Table 5: Summary of Results

Bar	**L (mm)**	$\frac{L}{r}$	$P_{cr,theo}$ **(kN)**	$P_{cr,exp}$ **(kN)**	$\sigma_{cr,theo}$ **(MPa)**	$\sigma_{cr,exp}$ **(MPa)**	**% Error**
1	0.508	138.5640646	8.491637222	8.714670491	35.06202685	35.98293271	2.559285163
2	0.737	201.0269992	4.879857741	4.140410674	20.14896523	17.09578335	17.85926868
3	0.902	246.0330438	3.483685883	2.764173634	14.3841623	11.41329141	26.02992228
4	0.997	271.945615	3.051702318	2.262497347	12.60049927	9.341866671	34.88202858

4 Discussion

4.1 Results Discussion

The experimental results indicate that the critical load decreases as the length of the bar increases. This is consistent with theoretical predictions and can be attributed to the increase in the slenderness ratio as the length increases. The critical stress also decreases as the length increases, which is also consistent with theoretical predictions. The percentage error between the theoretical and experimental critical loads increases as the length increases. This is likely due to the increased sensitivity of the longer bars to environmental conditions and other factors that can affect the buckling behavior.

4.2 Sources of Error

The percentage errors indicate variations between theoretical predictions and experimental results. Factors such as:

- **Environmental Conditions:** Variations in temperature, humidity, or other environmental factors can impact material behavior and measurements.
- **Alignment Issues:** Misalignment of experimental setup components, such as the load application system or displacement transducer, can lead to inaccuracies.
- **Instrumentation Limitations:** The precision and accuracy of measuring instruments, such as the load cell or displacement transducer, can introduce errors.
- **Boundary Conditions:** Deviations from idealized boundary conditions, such as perfectly pinned ends, can affect the buckling behavior.
- **Friction Effects:** Friction at the support points or between components can influence the buckling behavior.

Add to the errors between the theoretical and experimental results.

Despite discrepancies, the experiment successfully demonstrated the buckling behavior of slender pin-ended bars and provided insights into the accuracy of theoretical predictions. Future work could focus on refining experimental procedures and addressing sources of error for improved accuracy in theoretical-experimental comparisons.

5 Conclusions

The objectives of the experiment were successfully achieved. The buckling behavior of slender pin-ended bars was investigated and quantified through experimental procedures. The relationship between applied loads and the resulting center deflections for each tested bar was analyzed. The theoretical critical loads for the pin-ended bars were assessed and calculated using relevant analytical models. Experimental tests were performed to determine the critical loads for each bar. A comprehensive comparison between the theoretical predictions and the experimentally obtained critical loads for all tested bars was conducted. The experiment enhanced our understanding of the buckling behavior of slender pin-ended bars and evaluated the accuracy of theoretical predictions in relation to practical experimental outcomes.